SAMI3/WACCM-X Simulations of the Ionosphere during 2009

S. E. McDonald[1], F. Sassi[1], A. J. Mannucci[2]

[1]S. E. McDonald, Space Science Division, Naval Research Laboratory, Washington, DC, USA. (sarah.mcdonald@nrl.navy.mil)
[1]F. Sassi, Space Science Division, Naval Research Laboratory, Washington, DC, USA. (fabrizio.sassi@nrl.navy.mil)
[2]A. J. Mannucci, Jet Propulsion Laboratory, California Institute of Technology, Pasadena, CA, USA. (anthony.j.mannucci@jpl.nasa.gov)

Abstract

To study the day-to-day effects of the lower atmosphere on the ionosphere, we have performed simulations of SAMI3, NRL's physics-based model of the ionosphere, with a one-way coupling to the extended version of the Whole Atmosphere Community Climate Model (WACCM-X). WACCM-X has a top boundary located in the upper thermosphere (2.5×10^{-9} hPa, or ~500 km altitude); therefore we are able to drive SAMI3 using the full profile of the WACCM-X winds. To simulate specific events, WACCM-X can be constrained by data analysis products or observations. In this study, lower atmospheric weather patterns are introduced into WACCM-X using a linear combination of NASA's MERRA and the U.S. Navy's NOGAPS data assimilation products. The SAMI3/WACCM-X simulations are performed for several months in 2009. The January – February period is particularly interesting due to the large stratospheric warming event that occurred on 24 January 2009. We quantify the longitudinal and day-to-day ionospheric variability and compare our simulations with JPL ionospheric maps of total electron content.

1. Introduction

It has long been suspected that the lower atmosphere has a profound influence on the ionosphere. Day-to-day and longitudinal variability of the ionosphere not associated with geomagnetic activity has been attributed to processes originating in the lower atmosphere including tides, planetary waves, gravity waves, and even infrasound. While meteorological sources have been cited as the origin of much of the day-to-day variability in the ionosphere, only recently have we begun to understand the mechanisms connecting the lower atmosphere to the ionosphere [e.g. *Immel et al.*, 2006]. It is now recognized that upward-propagating tides, planetary waves and gravity waves can couple into the ionosphere through modification of thermospheric composition, influences on *E* region conductivities, modulation of thermospheric temperature and wind structure, and generation of electric fields through dynamo action [*Forbes et al*., 2000].

Though modeling and observational studies are beginning to reveal aspects of day-to-day ionospheric variability due to the lower atmosphere, we are only in the early stages of understanding which components of the lower atmosphere contribute to the observed variations. To investigate sources of day-to-day variability, we use an ionospheric model coupled with winds from a whole atmosphere model to study the period between January and February 2009. This is a geomagnetically quiet time but it is also characterized by a major sudden stratospheric warming on 24 January. We compare our model results with global ionospheric maps of TEC.

2. Models and Data

2.1 SD-WACCM-X

The Whole Atmosphere Community Climate Model (WACCM) is a build option of the *National Center for Atmospheric Research* (NCAR) Community Earth System Model version 1 (CESM1) and can be used in place of the standard atmospheric model. In its standard configuration, WACCM has 66 vertical levels from the ground to about 5.9×10^{-6} hPa (~140 km geometric height). WACCM can be configured into an extended version (WACCM-X) that incorporates all the features present in the regular configuration with the top boundary located in the upper thermosphere (2.5×10^{-9} hPa, or ~500 km altitude). WACCM-X can be used to simulate specific events by constraining the model meteorology with data analysis products or observations, using specified sea surface temperature at the lower boundary, and reconstructed spectral irradiances for the historical periods. We refer to this particular model configuration as specified dynamics WACCM-X (SD-WACCM-X). In this model configuration the winds and temperature are relaxed toward a set of analysis or observations. These atmospheric specifications are a combination of NASA/MERRA up to about 30 km and Navy's NOGAPS-ALPHA up to 92 km.

2.2 SAMI3

SAMI3 (Sami3 is A Model of the Ionosphere) is a comprehensive, three-dimensional, physics-based model of the ionosphere developed at the *Naval Research Laboratory* (NRL). SAMI3 is based on SAMI2 [*Huba et al*., 2000], a two-dimensional model of the ionosphere. SAMI3 models the plasma and chemical evolution of seven ion species (H^+, He^+, N^+, O^+, N_2^+, NO^+ and O_2^+) in the altitude range extending from 85 km to ~8 Re and latitudes up to ±88°. Currently, the magnetic field in SAMI3 is represented by an offset, tilted dipole. SAMI3 includes a potential solver to self-consistently solve for the electric fields [*Huba et al*., 2008]. Solar extreme ultraviolet (EUV) irradiances are determined from the NRL Solar Spectral Irradiance (NRLSSI) model [*Lean et al*., 2011]. In its standard configuration, SAMI3 uses NRLMSIS [*Picone et al*., 2003] to specify thermospheric composition and neutral temperature. The zonal and meridional horizontal winds are typically specified from climatology, such as HWM07 [*Drob et al*., 2008] or the updated HWM14 [*Drob et al*., 2015]. To introduce day-to-day variability into SAMI3, we use hourly winds provided by output from the SD-WACCM-X as described above.

2.3 Simulations

Each set of runs is performed for the month of January 2009, where we use the daily *Ap* and $F_{10.7}$ for each day. During this exceedingly quiet month, the median *Ap* is 4, with a maximum of 11; the median $F_{10.7}$ is 67 sfu and ranges from 66 to 69 sfu. Because NRLMSIS does not reproduce the anomalously low thermospheric density of the recent solar minimum, scalar parameters are applied to the composition and temperature profiles to match global mass density measurements derived from orbital data [*Emmert et al*., 2008]. We use a scalar of 0.96 for the temperature, 0.77 for oxygen and 0.93 for all other constituents.

We perform three sets of simulations with different winds. The first set uses HWM14 and serves as the climatological run. The second set of simulations is performed using SD-WACCM-X, which includes both migrating and non-migrating tides. In the third set of runs, we filter out

the most significant non-migrating tides from the SD-WACCM-X wind profiles; removed tides include DE1, SE1, SW1, DE2, SE2, DW2, and TE3.

3. Results

The most important process controlling the large-scale distribution of plasma in the low latitude region is the zonal (east-west) dynamo electric field that drives a vertical $\boldsymbol{E}\times\boldsymbol{B}$ drift of *F* region plasma at the equator. During the daytime, due to the high conductivity in the *E* region ionosphere, the global *E* region winds and tides control the electric field that leads to an uplift of plasma at the magnetic equator. Subsequent diffusion down the field lines, aided by gravity, results in bands of enhanced plasma density on either side of the magnetic equator are collectively called the Equatorial Ionization Anomaly (EIA), and show prominently in the global TEC. Models of tides that reach *E* region altitudes have been shown to significantly modulate the zonal electric fields and thus the $\boldsymbol{E}\times\boldsymbol{B}$ drift and EIA [*Hagan et al.*, 2007; *England et al.*, 2008]. Thus, by looking at the TEC and $\boldsymbol{E}\times\boldsymbol{B}$ drifts of our simulations, we illustrate how the neutral winds affect the ionosphere.

Before considering day-to-day variations of the ionosphere, we first consider the average behavior in January 2009 so that we can examine the extent to which the SAMI3 simulations reproduce major features associated with tides originating in the lower atmosphere. In Figure 1a, we show the JPL TEC at a constant local time (1400 LT) averaged over the ten day period, 6 – 15 January 2009. The mid to late afternoon is typically the time period during which the EIA is strongest, due to the integrated effect of the upward vertical plasma drifts over the previous several hours. The longitudinal structure varies from day to day, but averaging over multiple days reveals a wave-3 pattern in the longitudinal structure of the EIA. This wave-3 feature has been observed during northern winter in previous studies [e.g. *Scherliess et al.*, 2008; *Kil et al.*, 2008] and is primarily attributed to the DE2 non-migrating tide.

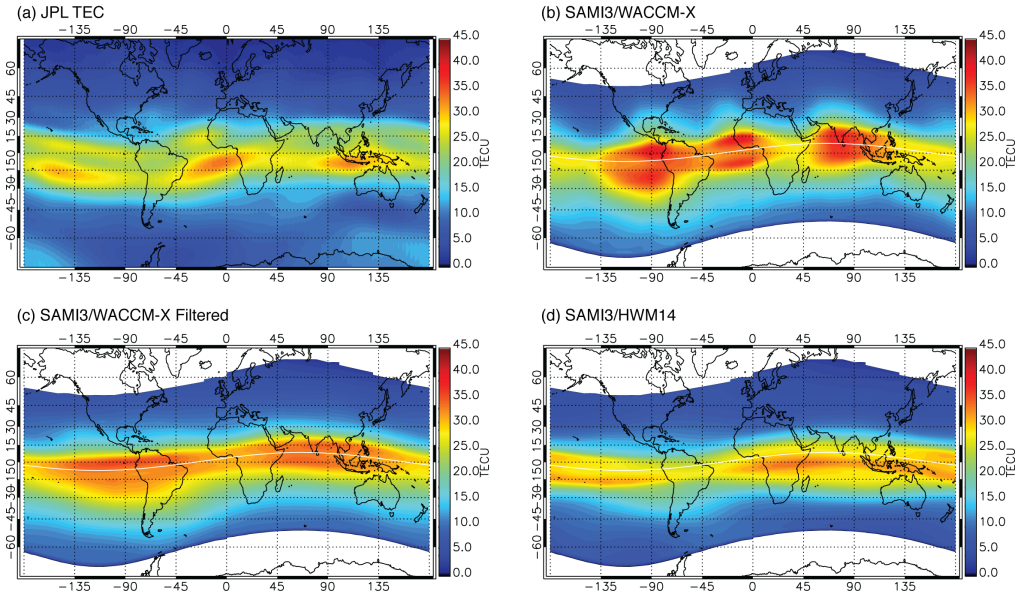

Figure 1. *Mean TEC at 1400 LT on 6 – 15 January 2009 for (a) JPL TEC maps, (b) SAMI3 with WACCM-X winds, (c) SAMI3 with filtered WACCM-X winds, and (d) SAMI3 with HWM14.*

Figures 1b-d show the SAMI3 TEC at 1400 LT averaged over 6 – 15 January 2009 for the simulations with (b) SD-WACCM-X winds, (c) SD-WACCM-X filtered winds, and (d) HWM14. In comparison with the JPL TEC (Figure 1a), the simulation with SD-WACCM-X winds (Figure 1b) reproduces the wave-3 feature in the EIA, albeit with some shifts in the strength and location of the crests. When the non-migrating tides are removed from the winds (Figure 1c), the wave-3 pattern disappears; the remaining longitudinal variation is associated with the offset of the geographic and magnetic equators [*McDonald et al*., 2008]. We can directly compare this result to the SAMI3 simulations using HWM14 winds (Figure 1d), since HWM14 does not include a parameterization for non-migrating tides. To first order, the filtered SD-WACCM-X winds produce similar results HWM14 and offers assurance that the SD-WACCM-X wind climatology is reasonable. We note, however, some differences in the longitudinal variation produced by the SD-WACCM-X winds versus HWM14. The HWM14 winds also better reproduce the asymmetry in the northern and southern EIA crests, as seen in the JPL TEC.

Figure 2b presents the SAMI3/SD-WACCM-X mean vertical plasma drift for 6 – 15 January 2009 at 300 km altitude. The SAMI3/SD-WACCM-X daytime drifts exhibit a wave-3 longitudinal structure peaking at about 10 LT. This structure is consistent with the vertical drift climatology for northern winter based on ROCSAT-1 observations [*Fejer et al*., 2008; *Kil et al*., 2008]. Figure 2c shows the drifts for the filtered wind simulation. Without the non-migrating tides, the wave-3 structure disappears and the peak daytime drift shifts to 12 LT. A comparison of Figure 2c to 2b shows that the longitudinal variations generated by non-migrating tides extends to all local times, including the early evening hours in which a pre-reversal enhancement (PRE) of the drifts, largely associated with the *F* region wind dynamo [*Millward et al*., 2001], is often observed. The pronounced longitudinal variations in the nighttime drift patterns suggest that the *F* region WACCM winds are strongly modulated by the non-migrating tides. The reduced longitudinal variation in the drifts associated with the filtered winds is similar to the drifts produced with HWM14 (Figure 2d) and is compared with the Scherliess-Fejer (SF) vertical drift model [*Scherliess and Fejer*, 1999] (Figure 2a). Overall, these summary figures show that SAMI3, when driven with SD-WACCM-X winds, captures the longitudinal variations associated with non-migrating tides.

Having established the average behavior of the ionosphere in January prior to the SSW, we now address the day-to-day variability at the time of the large stratospheric warming event of 24 January 2009. The goal is to describe the changes of day-to-day variability induced by the meteorological winds during a dynamically disturbed time and compare to simulations that use the climatological (HWM14) and filtered winds. Such comparisons evince the strong and statistically relevant influence of meteorological winds in general.

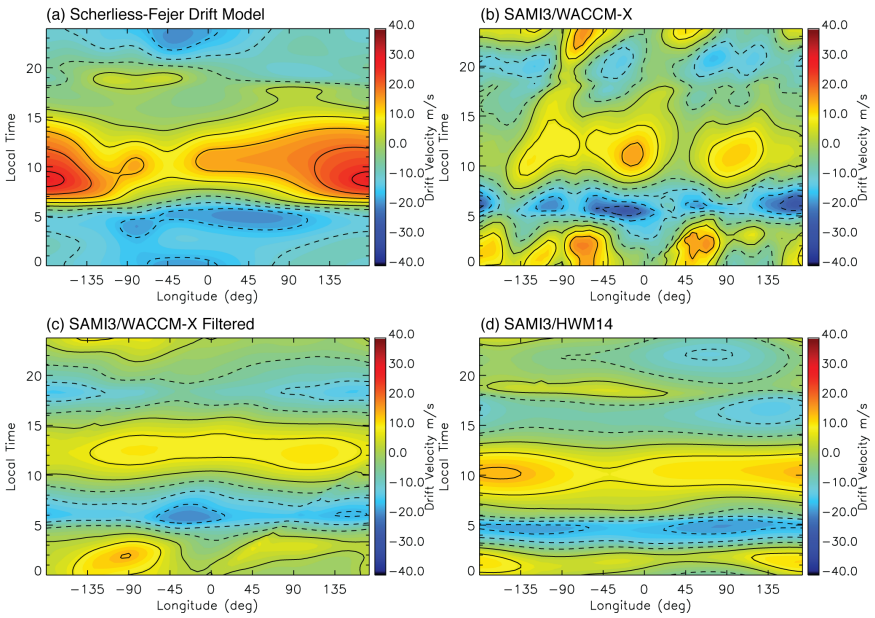

Figure 2. *Mean vertical **E×B** drifts as a function of geographic longitude and local time at the magnetic equator and 300 km altitude on 6 – 15 January 2009 for (a) the empirical Scherliess-Fejer drift model, (b) SAMI3 with WACCM-X winds, (c) SAMI3 with filtered WACCM-X winds, and (d) SAMI3 with HWM14.*

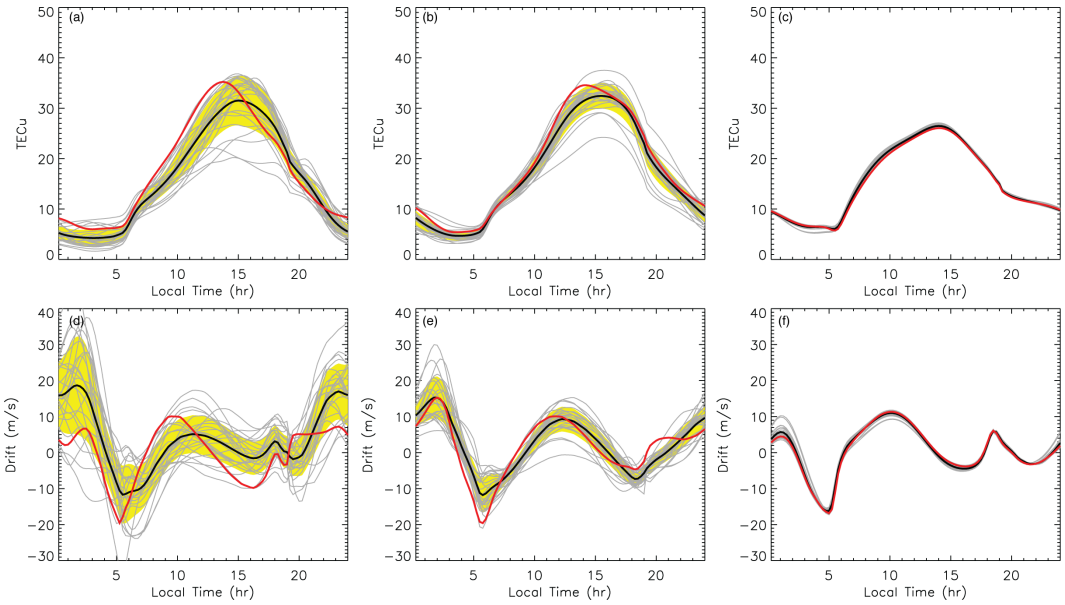

Figure 3. *(top row) TEC at the Jicamarca longitude (285° E, 0° N) as a function of local time for (a) SAMI3 with WACCM-X winds, (b) SAMI3 with filtered WACCM-X winds, and (c) SAMI3 with HWM14. (bottom row) (d-f) Vertical **E×B** drifts at the same location for the same simulations as in (a-c). The gray lines show the TEC and vertical drift for each day between 6 – 31 January 2009. The thick black line is the mean over this period, and the thick red line indicates the value on 27 January 2009 after the SSW event.*

Figure 3 illustrates the day-to-day variability of TEC and $\boldsymbol{E}\times\boldsymbol{B}$ vertical drifts at the magnetic equator for the three sets of SAMI3 simulations during 6 – 31 January 2009. TEC at the Jicamarca longitude (285° E), in the northern EIA crest at the geographic equator, is shown in the top row. In the bottom row, the vertical plasma drifts are shown at the magnetic equator and 300 km altitude. The black line represents the average behavior for this period and the red line indicates the TEC and drift pattern for 27 January 2009 a few days after the SSW event. Individual days are shown in grey and the yellow shaded area denotes the 1-sigma standard deviation. Considerable day-to-day variability is exhibited by the TEC and vertical drifts in the SAMI3/SD-WACCM-X simulation that includes both migrating and non-migrating tides (Figure 3a,d). The largest variation in TEC occurs at 1500 LT, when the density peaks, with a standard deviation of ±5 TECu (which corresponds to a variation of ±16% about the mean). The variation in the vertical drift is more uniform throughout the daytime hours and has a 1-sigma standard deviation of 5 m s^{-1}. The variability decreases by about one half when the non-migrating tides are removed (Figure 3b,e) and nearly disappears altogether in the SAMI3/HWM14 climatological simulations (Figure 3c,f). We note that the SAMI3/SD-WACCM-X simulations exhibit significant variability in the nighttime drifts, and will be addressed in more detail in the Discussion section below.

Goncharenko et al. [2010] reported on observations of the ionospheric response to the large stratospheric warming on 24 January 2009. The vertical drift recorded by the Jicamarca incoherent scatter radar (12° S, 285° E) indicated larger than average upward drifts in the morning hours and downward drifts in the early afternoon hours on 27 January 2009, a few days after the peak in the SSW in the stratosphere. In Figure 3a the red curve shows a similar pattern to the Jicamarca observations. The daytime drift peaks at 10:00 LT and turns negative after 12:00 LT. The simulated result lacks the amplitude of the observed drift (cf. Figure 1e in *Goncharenko et al*., [2010]), but the phase of the perturbation matches the observations quite well. When the nonmigrating tides are removed (Figure 3b) the feature nearly disappears; thus, in our simulations, the nonmigrating tides are the main driver of the perturbation on 27 January at the Jicamarca longitude.

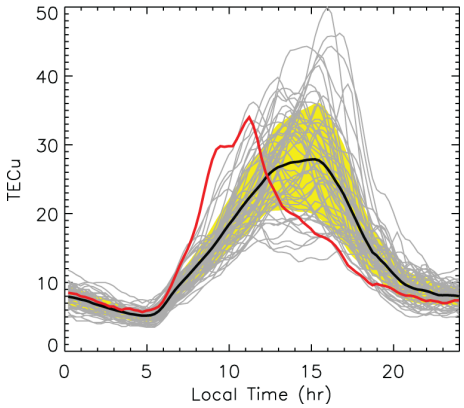

Figure 4. *JPL TEC at the Jicamarca longitude (285° E, 0° N) as a function of local time for days between 6 – 31 January 2009. The gray lines show TEC on each day, the thick black line is the mean TEC over this period, and the thick red lines indicates the TEC on 27 January 2009.*

For reference, we show the JPL TEC (0°N, 285°E) in Figure 4 for the January days. As with the SAMI3 simulations, the maximum TEC occurs at 1500 LT. The 1-sigma standard deviation is ±5 TECu, which corresponds to 30% variability, nearly twice that of the SAMI3

simulations. The SSW day shows a marked departure from the average behavior over the month. Daytime TEC sharply increases in the early morning hours, peaking just after 1100 LT, then rapidly declines in the afternoon as the $\boldsymbol{E}\times\boldsymbol{B}$ drift reverses direction. Whether or not the 27 January perturbation is directly associated with the SSW event is difficult to determine; the day-to-day variability is quite large, and the response after the SSW (red line) is only modestly larger than the day-to-day variability during this period, and therefore of dubious statistical significance.

An analysis of the neutral winds indicates the DE2, DE3, SE2 and SE3 tides are significant during this time. Though beyond the scope of this short paper, we note that the DE2 and DE3 decrease in amplitude around the time of the SSW event, while there is an amplification in the semidiurnal tides (SE2 and SE3) that are possibly responsible for the semidiurnal behavior in the TEC and vertical $\boldsymbol{E}\times\boldsymbol{B}$ drift velocity at the Jicamarca longitude. The actual physical mechanism responsible for this coupling remains unclear, and it may be due to the development of anomalous meridional gradients of the zonal flow at the times around an SSW [*McLandress*, 2002; *Sakazaki et al*., 2013].

5. Conclusions

In this study we have performed SAMI3 simulations of the ionosphere for January - February 2009 using winds from SD-WACCM-X that have been constrained by meteorological reanalysis. Additional runs during the same time period are performed for SD-WACCM-X winds with the non-migrating tidal components removed, and a climatological run was performed using HWM14. Using our model simulations, we have looked at the impact of lower atmospheric tides on the structure and variability of the ionosphere. We also characterized ionospheric variability due to the SSW event on 24 January 2009. Our conclusions are summarized as follows:

1. DE2 and DE3 non-migrating tides play an important role in the longitudinal structure of the low-latitude ionosphere and are mainly coupled in through the electrodynamics in the *E* region ionosphere via modulation of the vertical $\boldsymbol{E}\times\boldsymbol{B}$ drift. When averaged over several days, a combination wave-3/wave-4 pattern emerges; the JPL TEC over the same period (6 – 15 January 2009) indicates a wave-3 pattern is dominant, suggesting the DE3 in WACCM-X is too strong. SAMI3 simulations with the SD-WACCM-X filtered winds (migrating tides only) compare well with the climatological (HWM14) runs. So, while there is ample room for improvement, our results show that the SD-WACCM-X winds with data assimilation up to 92 km are reasonable.
2. We looked at the day-to-day variability of the ionosphere in January 2009 at the Jicamarca longitude and found that TEC varies by 16%. About half of this variation is due to non-migrating tides, with the other half due to the migrating tides. Only 1% of the variation is due to solar and geomagnetic effects during this quiet period at extreme solar minimum. The model captures about half of the variability observed in the JPL TEC, which is 30%, and is partly due to the use of climatological quantities for neutral density and temperature. The modeled $\boldsymbol{E}\times\boldsymbol{B}$ drift exhibits day-to-day variation of 5 m s^{-1}, in agreement with other models driven with lower atmospheric meteorology. Again, this is half of the observed variation of 10 ms^{-1}.
3. The SSW event had a minor impact on the modeled ionosphere and is possibly due to the weak amplitude of the SW2 tide in SD-WACCM-X, which has been identified as a main driver in other coupled model simulations. However, we do detect a semidiurnal feature in the $\boldsymbol{E}\times\boldsymbol{B}$ drifts at the Jicamarca longitude on 27 January 2009 with characteristics that

match observations; the upward vertical drift is enhanced during the morning hours and turns negative in the afternoon. This feature is plausibly associated with the SE2 and SE3 non-migrating tides. Contributions from these tides lead to longitudinal variations in the SSW impact on the ionosphere.

Acknowlegements. This work is supported by the Chief of Naval Research through NRL base funding. FS was partially supported by NASA/LWS grant NNH12AT21I. This work was also supported in part by a grant of computer time from the DOD High Performance Computing Modernization Program at the US Navy DOD Supercomputing Resource Center (NAVO).

References

England, S.L., T.J. Immel, E. Sagawa, S.B. Henderson, M.E. Hagan, S.B. Mende, H.U. Frey, C.M. Swenson, and L.J. Paxton (2006), Effect of atmospheric tides on the morphology of the quiet time, postsunset equatorial ionospheric anomaly, *J. Geophys. Res.*, *111*, A10S19, doi:10.1029/2006JA011795.

Drob, D. P., et al. (2008), An empirical model of the Earth's horizontal wind fields: HWM07, *J. Geophys. Res*., *113*, A12304, doi:10.1029/2008JA013668.

Drob, D.P. et al. (2015), An update to the horizontal wind model (HWM): The quiet-time thermosphere, *Earth and Space Science*, accepted.

Emmert, J. T., J. M. Picone, and R. R. Meier (2008), Thermospheric global average density trends, 1967 – 2007, derived from orbits of 5000 near-Earth objects, *Geophys. Res. Lett.*, 35, L05101, doi:10.1029/2007GL032809.

Fejer, B. G., et al. (2008), Quiet time equatorial F region vertical plasma drift model derived from ROCSAT-1 observations, *Journal of Geophysical Research-Space Physics*, *113*(A5).

Forbes, J.M., S.E. Palo, and X. Zhang (2000), Variability of the ionosphere, *J. Atmos. Solar-Terr. Phys.*, *62*, 685-693.

Goncharenko, L. P., J. L. Chau, H.‐L. Liu, and A. J. Coster (2010), Unexpected connections between the stratosphere and ionosphere, *Geophys. Res. Lett*., *37*, L10101, doi:10.1029/2010GL043125.

Hagan, M. E., et al. (2007), Connections between deep tropical clouds and the Earth's ionosphere, *Geophysical Research Letters*, *34*(20).

Huba, J. D., G. Joyce, and J.A. Fedder (2000), SAMI2 (Sami2 is Another Model of the Ionosphere): A New Low-latitude Ionosphere Model, *J. Geophys. Res., 105*(A10), 23035-23053.

Huba, J. D., et al. (2010), Self-consistent modeling of equatorial dawn density depletions with SAMI3, *Geophysical Research Letters*, *37*.

Immel, T.J., E. Sagawa, S.L. England, S.B. Henderson, M.E. Hagan, S.B. Mende, H.U. Frey, C.M. Swenson, and L.J. Paxton (2006), Control of equatorial ionospheric morphology by atmospheric tides, *Geophys. Res. Lett*., *33*, L15108, doi:10.1029/2006GL026161.

Kil, H., et al. (2008), Wave structures of the plasma density and vertical E x B drift in low-latitude F region, *Journal of Geophysical Research-Space Physics*, *113*(A9).

McDonald, S. E., K. F. Dymond, and M. E. Summers (2008), Hemispheric asymmetries in the longitudinal structure of the low-latitude nighttime ionosphere, *J. Geophys. Res*., *113*, A08308, doi:10.1029/2007JA012876.

McLandress, C. (2002), Seasonal variation of the propagating diurnal tide in the mesosphere and lower thermosphere. Part II: The role of tidal heating and zonal mean winds. *J. Atmos. Sciences, 59,* 907-922.

Millward, G.H., I.C.F. Muller-Wodarg, A.D. Aylward, T.J. Fuller-Rowell, A.D. Richmond, and R.J. Moffett (2001), An investigation into the influence of tidal forcing on *F* region equatorial vertical ion drift using a global ionosphere-thermosphere model with coupled electrodynamics, *J. Geophys. Res*., *106*, A11, 24733-24744.

Picone, J. M., A. E. Hedin, D. P. Drob, and A. C. Aikin (2003), NRL-MSISE-00 Empirical Model of the Atmosphere: Statistical Comparisons and Scientific Issues, *J. Geophys. Res.*, doi:10.1029/2002JA009430.

Sakazaki, T., M. Fujiwara, and X. Zhang (2013), Interpretation of the vertical structure and seasonal variation of the diurnal migrating tide from the troposphere to the lower mesosphere. *J. Atmos. Sol-Terr. Physics, 105*, 66-80.

Scherliess, L., and B.G. Fejer (1999), Radar and satellite global equatorial *F* region vertical drift model, *J. Geophys. Res*., *104*, 6829.

Scherliess, L., D. C. Thompson, and R. W. Schunk (2008), Longitudinal variability of low-latitude total electron content: Tidal influences, *J. Geophys. Res*., *113*, A01311, doi:10.1029/2007JA012480.